Communication-Free Carrier Synchronization Method for Autonomously Operated Single-Phase Inverters in Parallel

Takumi Iwamoto
dept. of Science of Technology Innovation
Nagaoka University of Technology
Nagaoka, Japan
s225057@stn.nagaokaut.ac.jp

Hiroki Watanabe
dept. of Electrical, Electronics, and Information Engineering
Nagaoka University of Technology
Nagaoka, Japan
hwatanabe@vos.nagaokaut.ac.jp

Yuki Nakata
dept. of Social Design Engineering
National Institute of Technology, Kochi College
Nagaoka, Japan
nakata@ee.kochi-ct.ac.jp

Jun-ichi Itoh
dept. of Science of Technology Innovation
Nagaoka University of Technology
Nagaoka, Japan
itoh@vos.nagaokaut.ac.jp

***Abstract*— This paper proposes a novel carrier synchronization control method for single-phase inverters operating in parallel without communication. In autonomous distributed operation, circulating currents arise due to carrier asynchrony in parallel-connected inverters. The proposed method focuses on the active power component at the switching frequency. When carrier synchronization is achieved, the active power at the switching frequency becomes zero in parallel-connected inverters. The proposed method calculates the active power at the switching frequency using high-speed sampling, switching states, and the fast Fourier transform (FFT). The proposed method enables carrier synchronization without inter-unit communication. Experimental results demonstrate that the proposed method successfully suppresses circulating currents to less than 81.2% of the rated current in a three-inverter parallel system, validating its effectiveness.**

Keywords—Universal Smart Power Module (USPM), Parallel connection, Carrier synchronization, Autonomous distributed system.

I. Introduction

In recent years, the importance of power electronics technology has been increasing in pursuit of a sustainable society. Power converters play a crucial role in all stages of energy generation, supply, and utilization, and their demand continues to grow year by year. In particular, the expansion of renewable energy integration is driving a shift in power systems from conventional centralized architectures to distributed configurations. In such systems, high-performance power converters are essential for the efficient and stable control of variable energy sources such as photovoltaic and wind power [1], [2]. Moreover, the growing adoption of electric vehicles and energy storage systems is further increasing the demand for power converters, which are required to support functionalities such as bidirectional power conversion, fast charging, and regenerative braking. In recent years, research on high-frequency and high-voltage converters utilizing next-generation semiconductor materials, such as silicon carbide (SiC) and gallium nitride (GaN), has advanced rapidly, enabling further miniaturization and improved efficiency in power conversion systems. These technological innovations are expanding the application of power electronics beyond conventional industrial equipment to a wide range of fields, including consumer electronics, information and communication devices, and even aerospace systems.

The design of power electronics systems requires not only power circuit design but also the development of control algorithms, countermeasures for switching noise, thermal design considering heat generation, as well as mechanical design and EMC (Electromagnetic Compatibility) compliance. These elements are highly interdependent, and even a single design change can significantly impact the overall performance and reliability of the system. As a result, the development of power converters often involves repeated cycles of design consideration, prototyping, and evaluation over extended periods, leading to substantial time and cost requirements. In the coming years, the demand for power converters is expected to continue growing, accompanied by increasing requirements for performance, reliability, and efficiency. Therefore, there is an urgent need to establish new design methodologies and modular technologies that enable the rapid and cost-effective development and deployment of power conversion systems.

The Universal Smart Power Module (USPM) integrates all essential components of a power converter, including the main power circuit, gate drivers, noise filters, and controller, into a single compact module [3], [4], [5], [6]. To accommodate a wide range of applications, the main circuit within the USPM is available in various configurations, such as single-phase H-bridges, three-phase inverters, and isolated DC-DC converters. This modularity enables the implementation of any power conversion system by selecting and combining appropriate USPMs, thereby significantly reducing development time and costs. The overall system comprises multiple USPM units and a master controller that oversees the entire operation. Commands from the master controller are transmitted wirelessly, enabling

This work was supported by the Council for Science, Technology and Innovation (CSTI), the Cross-ministerial Strategic Innovation Promotion Program (SIP), and the 3rd period of SIP "Smart energy management system" Grant Number JPJ012207 (Funding agency: JST).

each USPM to function as an ideal arbitrary waveform power source that generates various voltages and currents according to the received instructions.

In power conversion systems using Universal Smart Power Modules (USPMs), large-current power conversion is achieved by connecting multiple USPMs in parallel. In such configurations, where autonomous distributed power converters are operated in parallel, circulating currents are known to occur due to carrier asynchronization. To address this, carrier synchronization methods using synchronization signal lines have been proposed [7], [8]. However, since USPMs rely on wireless communication between the master controller and each USPM, synchronization via wired connections is not feasible. Although wireless-based synchronization methods have been proposed in [9] and [10], wireless communication often suffers from low transmission speeds and limited reliability. Therefore, in USPM-based power conversion systems, a carrier synchronization method that does not rely on communication with the master controller or other USPMs is desirable.

Several communication-free carrier synchronization methods have been proposed in the literature [11], [12], [13], [14]. Ref. [11] synchronizes two inverters by calculating the carrier phase difference between them. Still, it is limited to a two-inverter configuration and cannot be applied to systems with three or more units. Ref. [12] performs carrier synchronization based on the phase information of the grid, but it is sensitive to fluctuations in grid frequency, which affects its stability. In [13], a method using a virtual oscillator is proposed; however, its synchronization accuracy is constrained by sampling errors. The approach in [14] achieves carrier synchronization based on peak current detection, but it synchronizes inverters sequentially, one by one. Consequently, when clock frequency mismatches exist, the synchronization accuracy degrades as the number of inverters increases.

This paper proposes a communication-free carrier synchronization method for two parallel-connected single-phase inverters using high-speed sampling. In the proposed control scheme, the USPM controller performs high-speed sampling to extract the switching frequency component of the inductor current and calculates the corresponding active power. When carrier synchronization is achieved, the phase difference between the square-wave voltage output from the inverter and the inductor current becomes 90°. Therefore, carrier synchronization is realized by controlling the phase difference such that the active power becomes zero. A new contribution of this paper is the establishment of a communication-free carrier synchronization method that is robust against noise and grid frequency fluctuations. Experimental validation with three parallel inverters demonstrated that the proposed method reduced circulating current by 81.2%.

II. UNIVERSAL SMART POWER MODULE (USPM)

The Universal Smart Power Module (USPM) is a proposed module based on the Power Electronics Building Block (PEBB) concept, aiming to significantly reduce the development time and cost of power conversion systems. Each USPM integrates all essential components of a power converter, including the main power circuit (available in various configurations such as H-bridge inverters, three-phase inverters, and isolated converters), noise filters, and a high-speed controller with communication capability. By simply selecting and combining appropriate USPMs based on the application, designers can construct power conversion systems flexibly and rapidly, thereby significantly reducing development time.

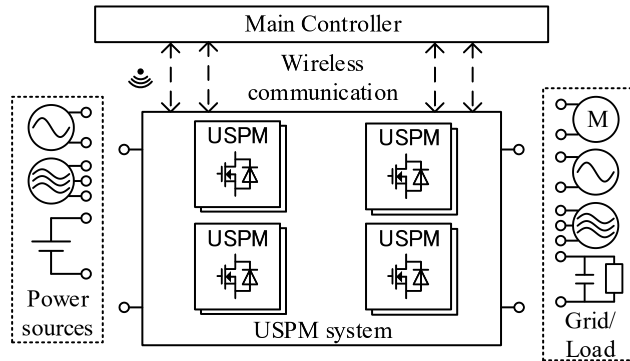

Fig. 1. Configuration of a power conversion system using USPMs. Each USPM integrates all essential components of a power converter and operates autonomously. Communication between USPMs is managed through a master controller.

Fig. 1 shows the configuration of a power conversion system based on the USPM concept. The system consists of a main controller and multiple USPMs. The main controller supervises all USPMs and transmits control commands, such as voltage or current references for feedback control, to the high-speed controller embedded in each USPM. Each USPM receives these commands and generates the required waveforms accordingly to perform power conversion.

Additionally, USPMs can be connected in series or in parallel, enabling their application in high-voltage and high-current systems. However, when multiple USPMs that operate autonomously are connected in parallel, as is the case in a USPM-based system, circulating currents may arise due to carrier asynchronization. Therefore, carrier synchronization is necessary to suppress these circulating currents.

III. CIRCUIT CONFIGURATION

Fig. 2 shows the circuit configuration of N single-phase inverters connected in parallel. This system assumes grid-connected operation and ω denotes the angular frequency of the grid. Each inverter is equipped with its controller and operates using bipolar modulation.

The current reference values are transmitted wirelessly from a master controller that supervises the entire system. Each inverter has an independent slave controller, which operates autonomously based on the command values provided by the master. In decentralized power converters, carrier asynchronization causes circulating currents to flow. These circulating currents increase the RMS value of the output current, making carrier synchronization essential.

IV. Circulating Current Analysis and Carrier Synchronization Method

A. Circulating Current Analysis

Fig. 3 shows the equivalent circuit on the output side of Fig. 1, focusing on the fundamental component of the carrier frequency. L_g represents the grid-side inductor, and the inductance of each inverter is assumed to be identical ($L=L_1=L_2=\ldots=L_N$). The proposed method targets the carrier frequency components, and resistive elements such as wiring resistance are negligible since they are sufficiently smaller than the inductive reactance. For simplicity, the circulating current is calculated based on the fundamental component of the carrier frequency. Additionally, the modulation index of the inverter is disregarded. ω_{SW} denotes the angular frequency of the carrier, and δ_2, δ_3, …, δ_N represent the carrier phase differences relative to $v1$. The current ix flowing through the x-th inverter output vx (x=1, 2, …, N) is given by

$$i_x = I_x \sin\left(\omega_{SW} t - \phi_x\right) \quad (1).$$

The amplitude I_x of the current i_x, and the phase lag angle ϕ_x are given by

$$I_x = \frac{V_{DC}}{\omega_{SW}\left(NLL_g + L^2\right)}\sqrt{A_{ix}^{\ 2} + B_{ix}^{\ 2}} \quad (2),$$

$$\phi_x = \arctan\frac{-B_{ix}}{\sqrt{A_{ix}^{\ 2} + B_{ix}^{\ 2}}} \quad (3).$$

A_{ix} and B_{ix} are given by

$$A_{ix} = \left(NL_g + L\right)\cos\delta_x - L_g\left(1 + \sum_{k=2}^{N}\cos\delta_k\right) \quad (4),$$

$$B_{ix} = \left(NL_g + L\right)\sin\delta_x - L_g\sum_{i=2}^{N}\sin\delta_x \quad (5).$$

Note that δ_1=0. The circulating current, i_{x_loop}, flowing through the x-th inverter is given by

$$i_{x\_loop} = \frac{1}{N-1}\sum_{i=1}^{N}\left(i_x - i_k\right) = \frac{1}{N-1}\frac{V_{DC}}{\omega_{SW}L}\left(C_{ix}\sin\omega_{SW}t - D_{ix}\cos\omega_{SW}t\right) \quad (6),$$

Where C_{ix} and D_{ix} are given by

$$C_{ix} = N\sin\delta_x - \sum_{k=2}^{N}\sin\delta_x \quad (7),$$

$$D_{ix} = N\cos\delta_x - 1 - \sum_{k=2}^{N}\cos\delta_x \quad (8).$$

When carrier synchronization is achieved ($\delta_2=\delta_3=\ldots=\delta_N=0$), both C_{ix} and D_{ix} become zero. Therefore, according to (6), the circulating current is eliminated. Furthermore, from (3), since B_{ix}=0 during carrier synchronization, the phase of the current concerning the voltage v_x is 90°.

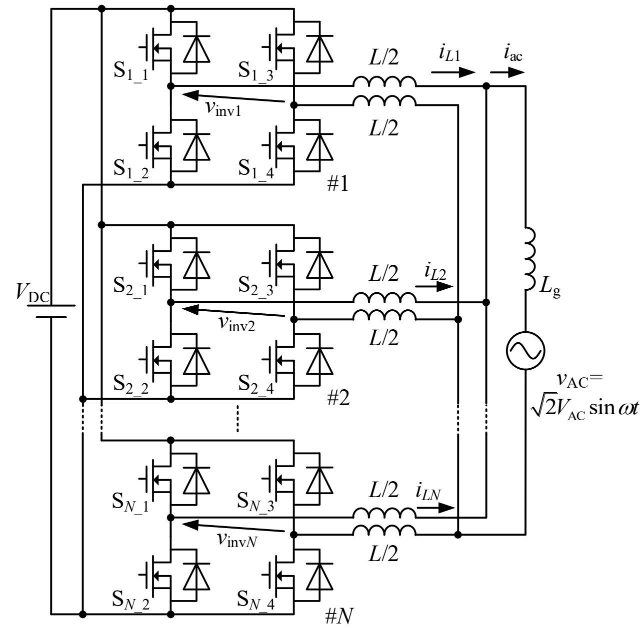

Fig. 2. Single-phase inverter with multiple units connected in parallel. ω is the angular frequency of the grid.

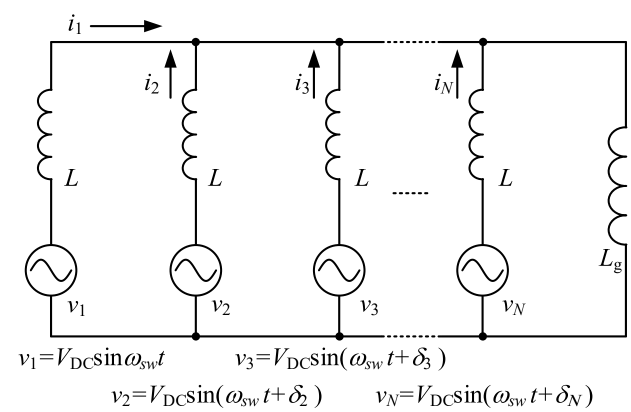

Fig. 3. Equivalent circuit of the carrier frequency components for a single-phase inverter with multiple units connected in parallel. i_1, i_2, i_3, …, i_N represent the carrier frequency component of the inductor current for each inverter, and δ_2, δ_3, …, δ_N is the carrier phase difference between v_1 and v_2, v_3, …, v_N.

The instantaneous power component at the carrier frequency can be represented by (9), where I_x and ϕ_x are used.

$$p_x = \frac{1}{2}V_{DC}I_x\left\{\cos\phi_x - \cos\left(2\omega_{SW}t - \phi_x\right)\right\} \quad (9).$$

Accordingly, the active (average) power over one carrier cycle is obtained as shown in (10).

$$P_x = \frac{1}{2}V_{DC}I_x\cos\phi_x \quad (10).$$

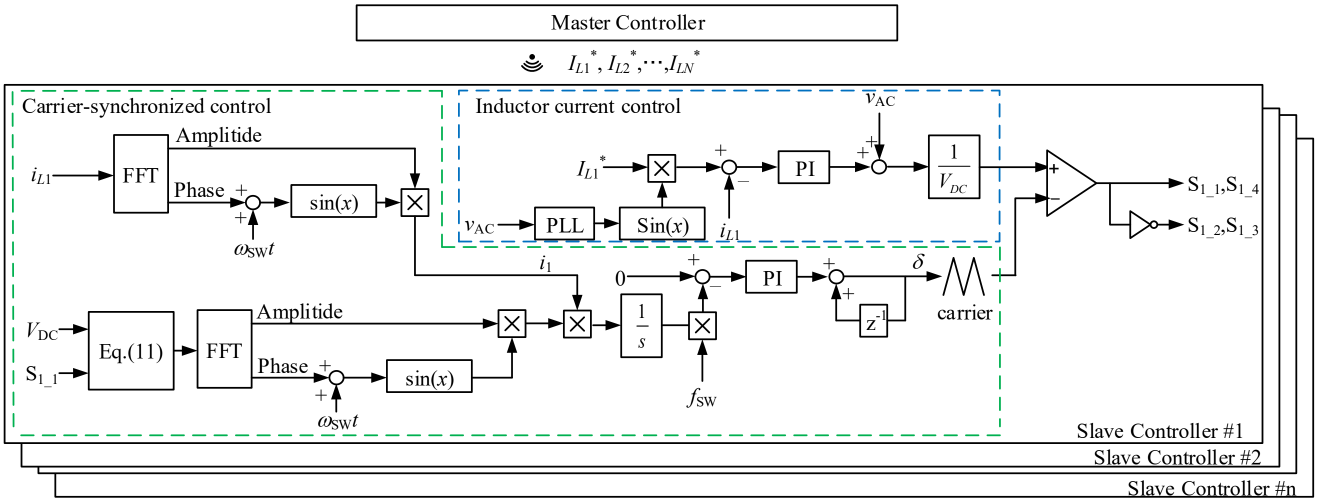

Fig. 4. Control block of proposed control. Inductor current control section is configured by PI control. The carrier synchronization control section consists of FFT, integrator, and PI control to operate the carrier phase.

Substituting ϕ_x=90° into (10) yields zero active power. This indicates that, under carrier-synchronized conditions, the power factor of the carrier frequency component becomes zero and the active power is eliminated. Therefore, by controlling the carrier phase angle of each inverter so that the active power becomes zero, the carrier phase difference δ_x can be adjusted to 0°.

B. Carrier Synchronization Method

Fig. 4 shows the control block diagram of the proposed carrier synchronization method for multiple inverters connected in parallel. Each inverter controls the inductor current using PI control based on the command values transmitted from the master controller. The proposed carrier synchronization control is applied to all inverters.

In the proposed carrier synchronization control, the amplitude and phase of the carrier frequency component are first obtained using an FFT based on the inductor current i_{Lx} and the inverter voltage v_{invx}. Note that v_{invx} is not measured directly, but is instead calculated from the DC voltage V_{DC} and the switching state using the following equation.

$$\begin{cases} v_{invx} = V_{DC} & \left(S_{1\_x} = 1\right) \\ v_{invx} = -1 & \left(S_{1\_x} = 0\right) \end{cases} \quad (1).$$

Next, the instantaneous power is calculated and integrated using the amplitude and s of the acquired ix and vinvx. The active power is then obtained by multiplying the integrated value by the switching frequency. The carrier phase angle is adjusted by PI control such that the calculated active power converges to zero. When the active power is positive, it indicates that the carrier phase is lagging relative to other inverters; when negative, it is leading. Therefore, carrier synchronization is achieved by advancing the carrier phase in the case of positive active power and delaying it in the case of negative active power. Here, the FFT and active power calculation are performed with a period that is an integer multiple of the carrier period, thereby reducing quantization error. The control period of the PI controller depends on the calculation period of the active power.

Since the proposed method utilizes only information locally available for each standalone inverter, such as the switching state, input voltage, and inductor current, it eliminates the need for communication with other inverters or with a master or slave controller. Furthermore, although high-speed sampling is generally sensitive to noise, the application of FFT to extract the switching-frequency component of the inductor current effectively mitigates its impact.

V. Experimental Verification

Table 1 shows the experimental conditions. Three inverters are connected in parallel, each with its own controller. The FFT is performed with 25 sampling points within one carrier period, and the computation is executed every 10 ms, corresponding to 100 carrier periods. A HAS-50-S current sensor is employed, with its 3 μs detection delay compensated in advance.

Fig. 5 shows the grid voltage, inductor current, and circulating current of i_{Lx} under rated operating conditions. Before enabling carrier synchronization control, the inverters are not synchronized, and a circulating current is observed. The RMS value of the circulating current in this condition is 6.69 A. Additionally, the amplitude of the circulating current varies with a period of approximately 4 seconds due to a continuous change in the carrier phase difference caused by a clock frequency mismatch. After enabling the carrier synchronization control, synchronization is achieved, and the circulating current is suppressed. The RMS value of the circulating current is reduced to 1.26 A, which corresponds to an 81.2% reduction achieved by the proposed method.

Fig. 6 shows the transient response waveforms observed during the operation of the carrier synchronization control. Before the control is activated, the carrier signals of each inverter are asynchronous, resulting in significant circulating currents among the parallel-connected inverters. These circulating currents cause an increase in the amplitude of the inductor currents, leading to higher current stress on the components and greater overall power loss. This is evident from the visibly large oscillations in the current waveforms. Once the carrier synchronization control is turned on, the carrier phases gradually begin to align. As a result, the circulating current i_{1_loop} is significantly reduced, and the amplitudes of inductor currents begin to decrease accordingly. This transition demonstrates the effectiveness of the proposed method in synchronizing the switching operation of each inverter without communication, thereby suppressing circulating currents and improving current quality.

Fig. 7 presents enlarged waveforms of the inductor current around the zero-crossing point of the grid voltage. Figure 6(a) shows the waveform when the carrier phase difference is significant. In this case, the voltage across the inductor changes multiple times within a single cycle due to phase mismatch, and the inductor current does not exhibit a triangular waveform. In contrast, Fig. 7(b) shows the waveform after synchronization. Since all inverters switch at nearly the same timing, the inductor current becomes nearly triangular. The average amplitude of the inductor current in Figs. 7(a) and 7(b) are 15.2 A and 5.45 A, respectively, indicating that the RMS current is also reduced.

VI. Conclusion

This paper proposed a communication-free carrier synchronization method for multiple autonomous single-phase inverters connected in parallel. In the proposed method, the carrier phase angle is controlled such that the active power of the carrier frequency component, calculated using high-speed sampling, becomes zero, thereby achieving carrier synchronization. The proposed control requires no information from other inverters and enables synchronization without communication between slave controllers or with a master controller. Although high-speed sampling is generally susceptible to noise, the use of FFT and integration in this method effectively suppresses the impact of noise. It was analytically demonstrated that, even in multi-inverter parallel operation, the active power becomes zero under carrier-synchronized conditions. Simulation results confirmed that the circulating current was suppressed to below 0.02 p.u. when five inverters were connected. Experimental validation showed that the proposed method reduced the circulating current by 81.2% compared to the asynchronous case. The proposed method operates effectively even at relatively low sampling frequencies, making it applicable not only to systems based on USPMs but also to a wide range of general-purpose parallel inverter systems.

Future work will focus on a detailed investigation of the impact of inductance variation and wiring resistance on carrier synchronization, as well as the relationship between sampling frequency and synchronization accuracy.

TABLE I. Experimental condition

Quantity	Symbol	Value
DC voltage	V_{DC}	200 V
Grid voltage	v_{AC}	100 V_{rms}
Grid frequency	f	50 Hz
Rated current of one unit	i_{L1}~i_{L3}	10 A_{rms}
Rated power of one unit	P_1~P_3	1 kW
Inverter side inductance	L_1~L_3	450 µH (%Z=1.4%)
Grid side inductance	L_g	640 µH (%Z=6.0%)
Switching frequency	f_{SW}	10 kHz
Sampling frequency	f_{samp}	250 kHz

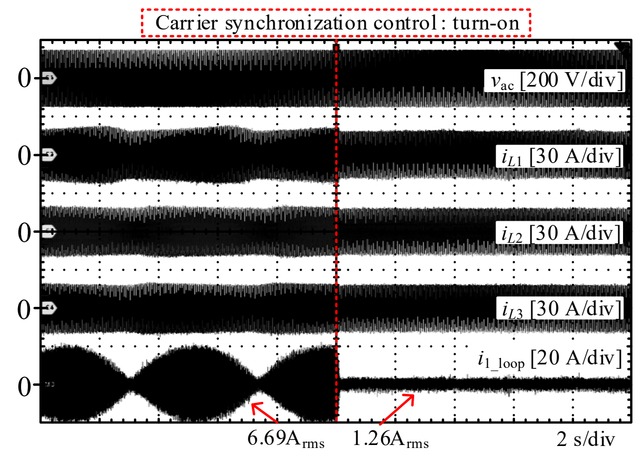

Fig. 5. Inductor current and circulating current waveforms.

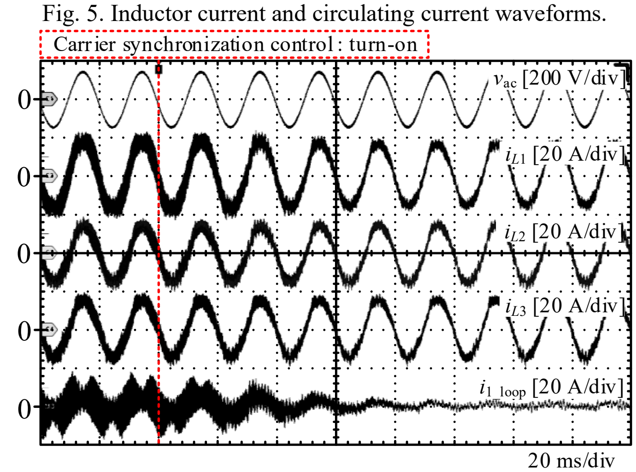

Fig. 6. Transient response waveform after carrier synchronization control is turn-on.

References

[1] Kazuki Ohuchi, Yuko Hirase, and Marta Molinas, “MIMO and SISO Impedance-based Stability Assessment of a Distributed Power Source Dominated System,” IEEJ Journal of Industry, Vol. 12, No. 4, pp. 653-663, 2023.

[2] M. M. Rajan Singaravel, and S Arul Daniel, “MPPT With Single DC–DC Converter and Inverter for Grid-Connected Hybrid Wind-Driven PMSG–PV System,” IEEE Transactions on Industrial Electronics, Vol. No. 8, pp. 4849-4857, August 2015.

[3] Hiroki Watanabe, Koki Yamanokuchi, Yoshinari Ikeda, Yoshikazu Takahashi, and Jun-ichi Itoh, “Universal Smart Power Module (USPM) for Carbon Neutral Society,” IEEE Transactions on Industry Applications, Vol. 60, No. 2, pp. 3411-3417, March/April 2024.

[4] Koki Yamanokuchi, Hiroki Watanabe, and Jun-ichi Itoh, “Distributed Control Method for Power Conversion System With Series-Connected Autonomous Modular Converters,” IEEE Transactions on Power Electronics, Vol. 38, No. 12, pp. 15242-15252, December 2023.

[5] Daiseke Hiroe, Xiaohan Zhang, Kazuki Nakamura, Kotaro Sato, Ryosuike Suzuki, Knataro Yoshimoto, and Tomoki Yokoyama, "A Study of 10MHz Multi-Sampling Deadbeat Control for PMSM Drive System using USPM Controller," IEEJ Journal of Industry Applications, Vol. 12, No. 3, pp. 508-516, 2023.

[6] Mana Sakamoto and Hitoshi Haga, "Control Method for Universal Smart Power Module Considering Wireless Communication," IEEJ Journal of Industry Applications, Vol. 12, No. 2, pp. 204-214, 2023.

[7] Max A. Parker, Li Ran, and Stephen J. Finney, "Distributed Control of a Fault-Tolerant Modular Multilevel Inverter for Direct-Drive Wind Turbine Grid Interfacing," IEEE Transactions on Industrial Electronics, Vol. 60, No. 2, pp. 509-522, February 2013.

[8] Youngsang Bae and Rae-Young Kim, "Suppression of Common-Mode Voltage Using a Multicentral Photovoltaic Inverter Topology With Synchronized PWM," IEEE Transactions on Industrial Electronics, Vol. 61, No. 9, pp. 4722-4733, September 2014.

[9] Wen-Qin Wang, "Carrier Frequency Synchronization in Distributed Wireless Sensor Networks," IEEE Systems Journal, Vol. 9, No. 3, pp. 703-713, September 2015.

[10] Qasim M. Chaudhari, "A simple and robust clock synchronization scheme," IEEE Transactions on Communications, Vol. 60, No. 2, pp. 328-332, February 2012.

[11] Tatsuya Kohara, Toshihiko Noguchi, Seiji Kondo, "Carrier Phase Error Detection Method and Synchronization Control of Parallel-Connected PWM Inverters without Signal Line," IEEJ Transactions on Industry Applications, Vol. 124, No. 5, pp. 450-456, 2004.

[12] Tao Xu, Feng Gao, Xiongfei Wang, and Frede Blaabjerg, "A Carrier Synchronization Method for Global Synchronous Pulsewidth Modulation Application Using Phase-Locked Loop," IEEE Transactions on Power Electronics, Vol. 34, No. 11, pp. 10720-10732, November 2019.

[13] Jian Hu and Hao Ma, "Synchronization of the carrier wave of parallel three-phase inverters with virtual oscillator control," IEEE Transactions on Power Electronics, Vol. 32, No.10, pp.7998-8007, October 2017.

[14] Jiakang Zhang, Dehong Zhou, Jianxiao Zou, Xin Liu, Hong Zhang, Zewei Shen, "Carrier Phase Synchronization Based on Circulating Current Identification for Distributed Inverters," IEEE Transactions on Power Electronics, Vol. 40, No. 8, pp. 10433-10442, August 2025.

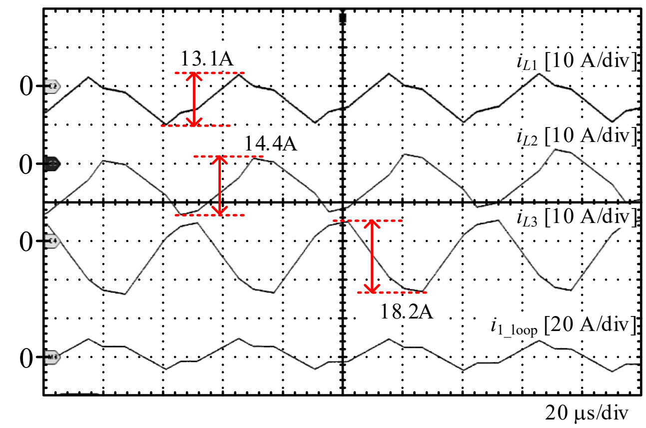

(a) Before carrier synchronization.

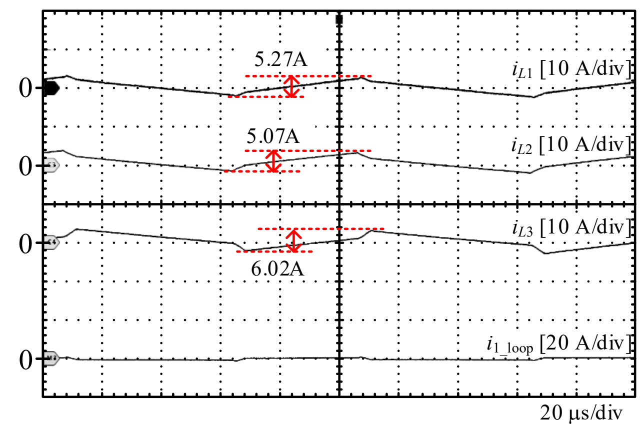

(b) After carrier synchronization.

Fig. 7. Magnified waveforms of inductor current and circulating current at zero cross of grid voltage.